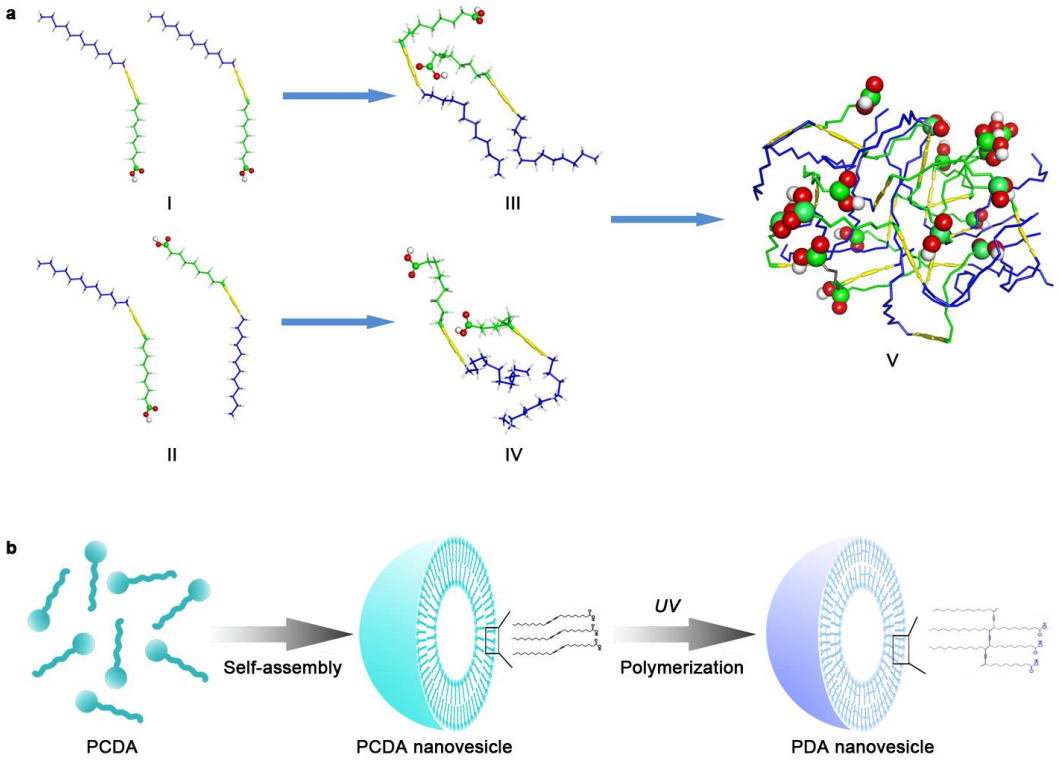

Supplementary Figure 1 | Preparation of PDA nanoparticles derived from self-assembly of PCDA. (**a**) Computer simulation on the self-assembly of PCDAs. Two kinds of totally different initial conformations were arranged for a cluster consisting of 2 PCDAs: head-head parallel (I) and head-tail parallel (II). In the simulation, PCDAs in a head-head parallel arrangement moved closer, and their polar heads pointed toward one direction while their hydrophobic tails pointed to the other direction (III). PCDAs in a head-tail parallel arrangement approached to each other and finally demonstrated a similar conformation to the former (IV). Thus, the initial conformation of PCDA cluster has little influence on the final simulated conformation. Moreover, another PCDA cluster consisting of 16 PCDAs was constructed by merging two 2-PCDA clusters, then two 4-PCDA clusters, and finally two 8-PCDA clusters sequentially. After the simulation, the polar heads of PCDAs were all exposed to solvent and their hydrophobic tails tended to be hidden within the inner of the cluster (V). The carbon atoms on the polar head of PCDA were colored with green, while those on hydrophobic tail of PCDA were colored with blue. Carbon atoms on the alkyne moiety were colored with yellow. (**b**) The preparation scheme of PDA nanoparticles. Assisted by sonication, PCDA self-assembled into nanovesicles, making PCDA closely packed and properly ordered. Then colourless PCDAs nanovesicles undergo polymerization via a 1,4-addition reaction to form alternating ene-yne polymer chains upon irradiation with 254 nm UV light, creating blue vesicle-structured PDA nanoparticles with a characteristic absorption peak at around 640 nm.

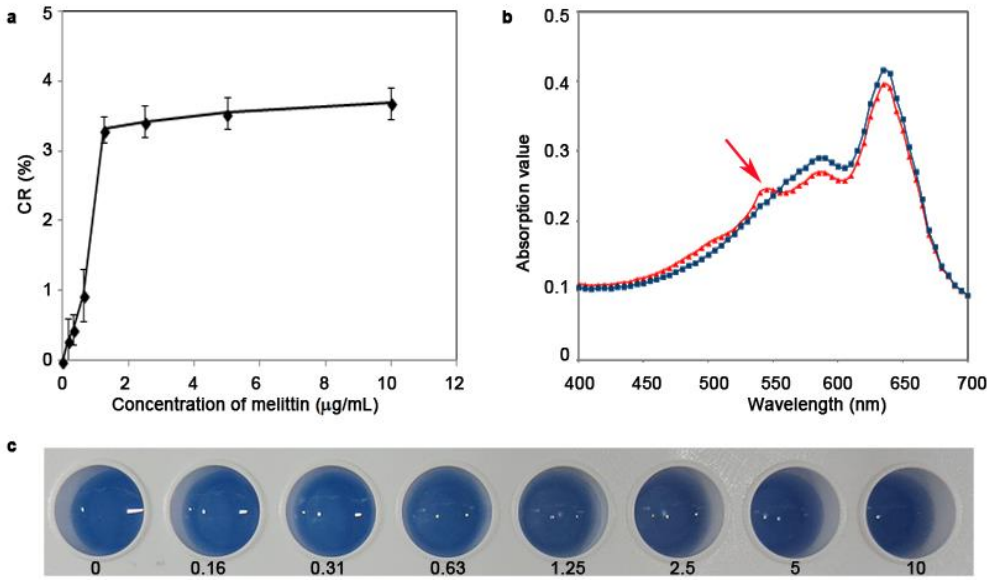

Supplementary Figure 2 | Melittin induced chromatic shift of PDAs. (**a**) The color response (CR) of PDA nanoparticles exposed to melittin at different concentrations; (**b**) The absorption curves of initial PDA nanoparticles (blue) and melittin incubated PDA nanoparticles. The red arrow indicated the slight color shift from blue to red. (**c**) The color shift of PDA nanoparticles upon exposure to melittin at different concentrations. By naked eye, we can observe the slight color shift of PDA nanoparticles after incubation with melittin. In this experiment, 100 μL of PDA nanoparticles solution (20 μg/mL) was incubated with100 μL of melittin solution at 37 ^{o}C for 30 min.

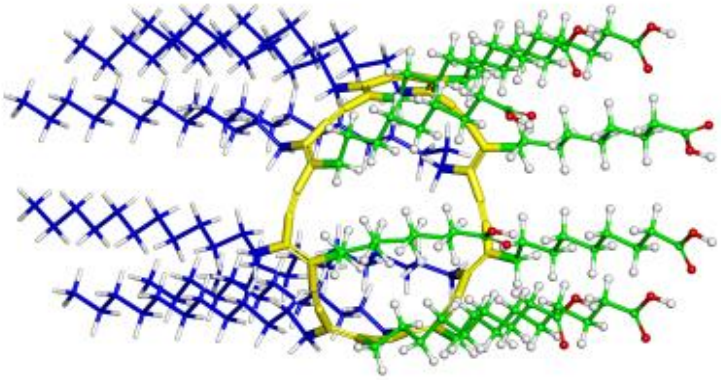

Supplementary Figure 3 | The computer simulated structure of PDA. It was constructed with Discover Studio 3.1 and optimized in Hyperchem workspace. The degree of polymerization is set as 8. The carbon atoms on the polar head of PCDA were colored with green, while those on hydrophobic tail of PCDA were colored with blue. Carbon atoms on the alkyne moiety were colored with yellow.

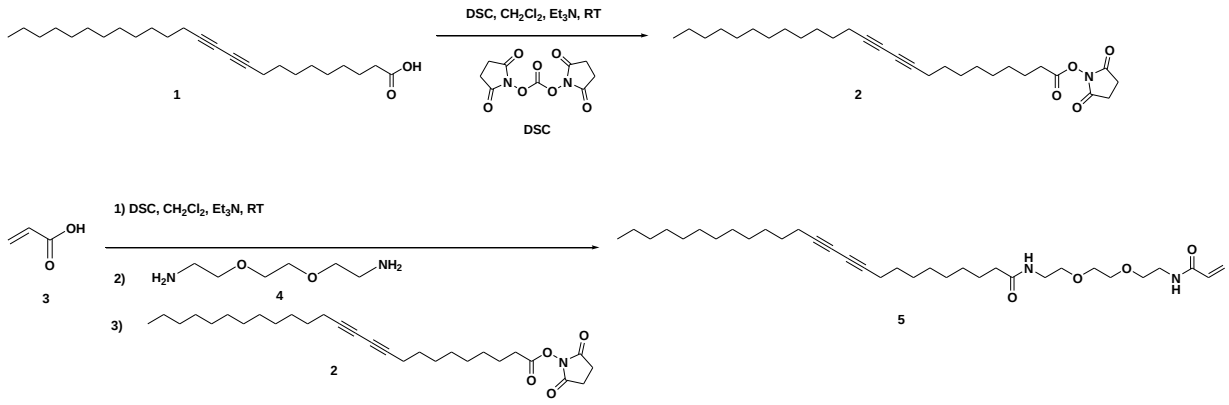

Supplementary Figure 4 | Preparation scheme of PCDA-A 5.

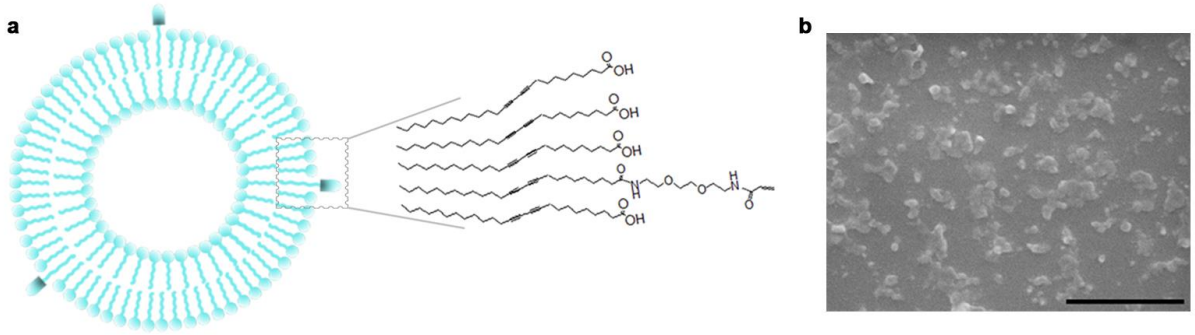

Supplementary Figure 5 | PCDA-A 5 and PCDA composite nanoparticles. (**a**) The schematic presentation of the surface groups of PCDA-A **5** and PCDA composite nanoparticles. By mixing PCDA and PCDA–A **5**, the resulting nanoparticle possessed acrylamide groups on its surface. (**b**) Scanning electron microscope image of PCDA-A **5** and PCDA composite nanoparticles. The scale bar is 1 μm.

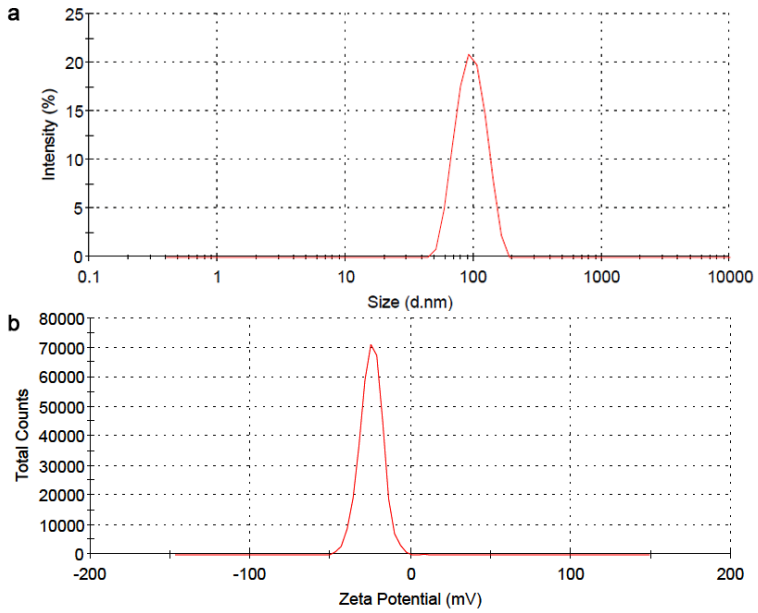

Supplementary Figure 6 | The particle size and zeta potential of PCDA-A and PCDA composite nanoparticles. (**a**) The particle size distribution spectrum. (**b**) The zeta potential distribution spectrum. These data were determined by Malvern Nano-ZS Instrument. The test temperature is 25 ^{o}C.

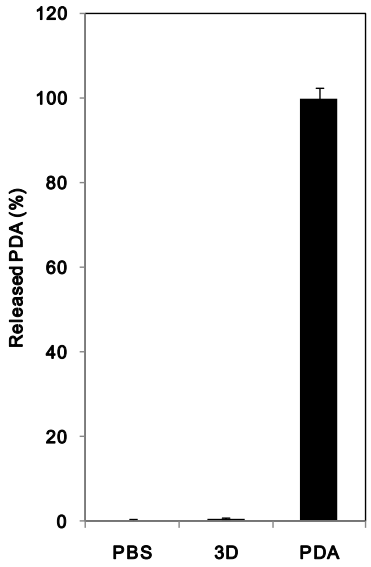

Supplementary Figure 7 | The release of PDA from the 3D detoxifier. After incubation of the 3D detoxifier in PBS for 24 hrs, the release of PDA was monitored by measuring the absorbance (A_{3D}) of the supernatant at 640 nm. Controls for 0 and 100% release consisted of PBS ($A_{0\%}$) and a solution with the same amount of PDA nanoparticles in the 3D detoxifier ($A_{100\%}$), respectively. The percentage of released PDA nanoparticles was calculated by $(A_{3D}\text{-}A_{0\%})\times(A_{100\%} - A_{0\%})^{-1}\times 100\%$.

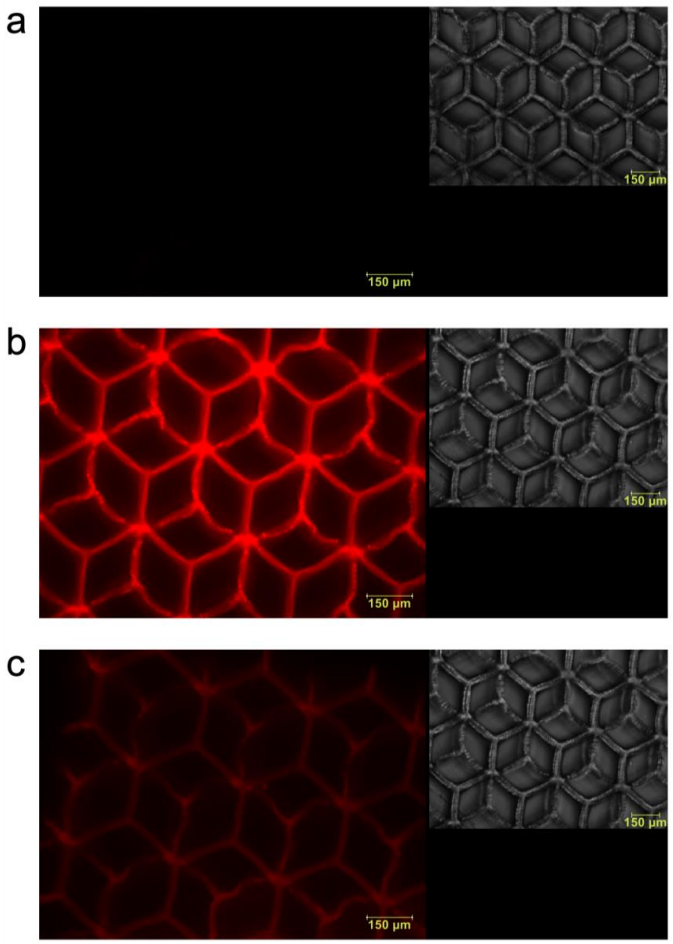

Supplementary Figure 8 | The diffusion of molecules into PEGDA hydrogel. After PEGDA hydrogel (10%) was incubated with TRITC-Dextran solution overnight, the supernatant was discarded and the image of the PEGDA hydrogel was taken. (a) Control with no Dextran, (b) 0.5 mg/mL TRITC-Dextran (4.4 kD) overnight incubation. (c) 0.5mg/mL TRITC-Dextran (65 kD to 85 kD) overnight incubation.

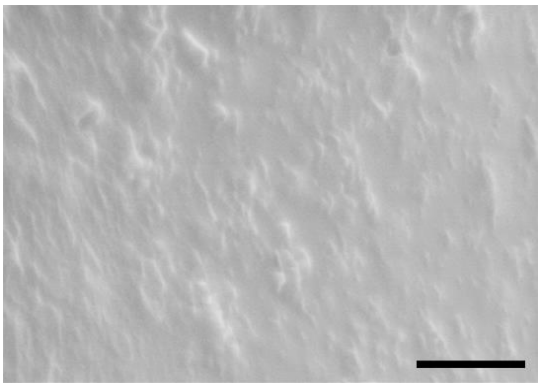

Supplementary Figure 9 | Scanning electron microscope image of the surface of the 3D detoxifier. The scale bar is 1 μm**.**

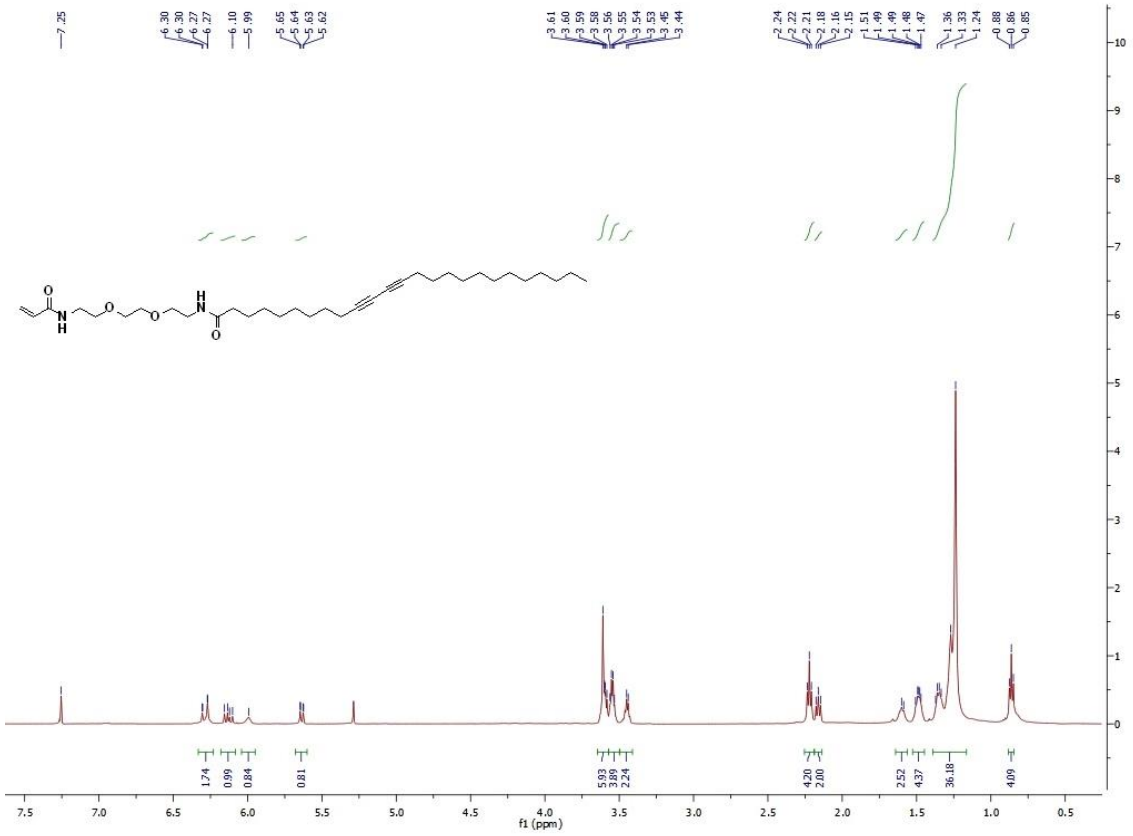

Supplementary Figure 10 | ^{1}H-NMR spectrum of PCDA-A 5. ^{1}H NMR (500 MHz, $CDCl_3$) δ 0.86 (t, *J* = 7.5 Hz, 3H), 1.24-1.36 (m, 36H), 1.48 (m, 4H), 1.65 (m, 2H), 2.16 (t, *J* = 7.5 Hz, 2H), 2.22 (t, *J* = 7.5 Hz, 2H), 3.45 (m, 2H), 3.57 (m, 4H), 3.60 (m, 6H), 5.63 (dd, *J* = 10, 5 Hz, 1 H), 5.99 (bs, 1H), 6.10 (m, 1H), 6.27-6.30 (m, 2H)

.

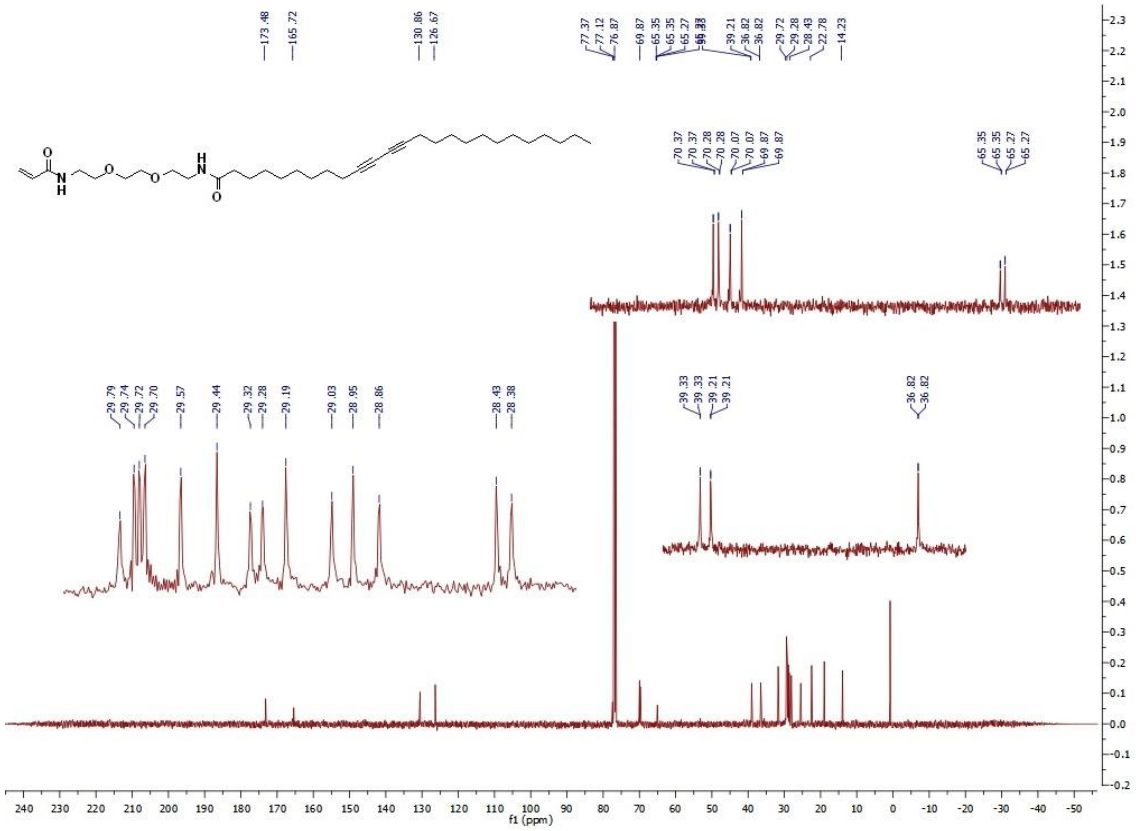

Supplementary Figure 11 | ^{13}C -NMR spectrum of PCDA-A 5. ^{13}C NMR (125 MHz, $CDCl_3$) δ 14.23, 19.28, 22.78, 25.78, 28.38, 28.43, 28.86, 28.95, 29.03, 29.19, 29.28, 29.32, 29.44, 29.57, 29.70, 29.72, 29.74, 29.79, 36.82, 39.21, 39.33, 65.27, 65.35, 69.87, 70.07, 70.28, 70.37, 126.67, 130.86, 165.72, 173.48.

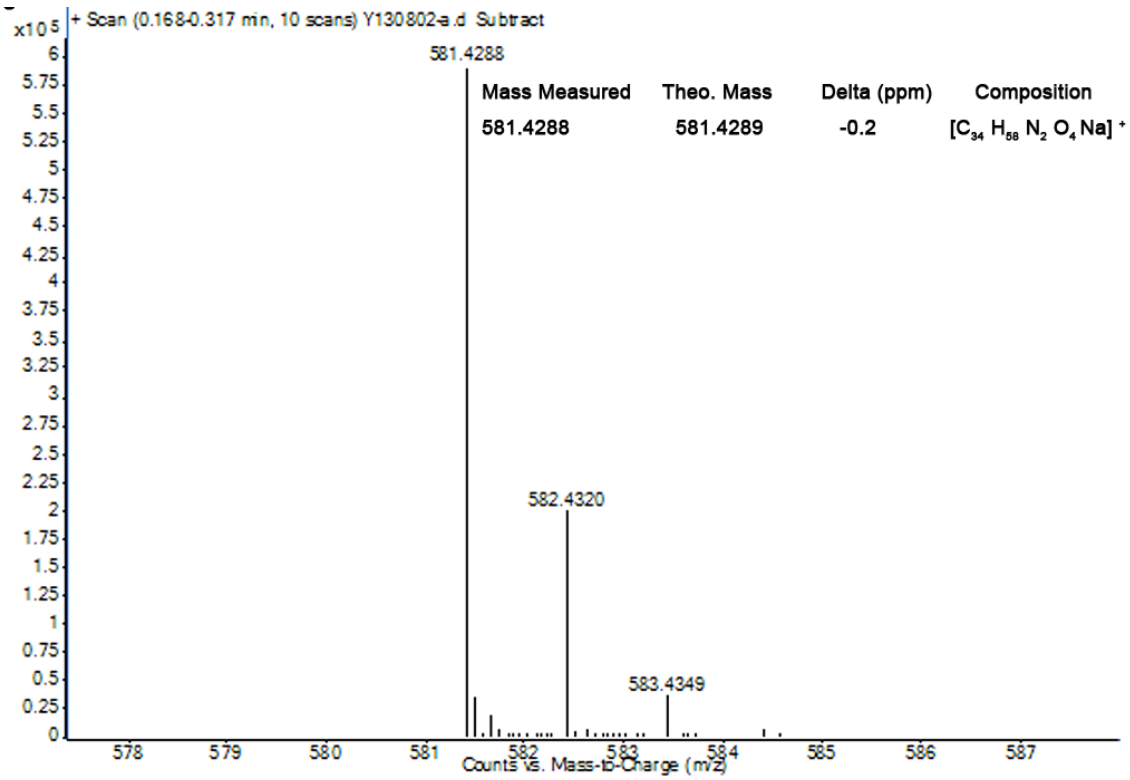

Supplementary Figure 12 | High resolution mass spectrum of PCDA-A 5. The peak at 581.4288 was founded in the high resolution mass spectrum, which was attributed to the compound $[C_{34}H_{58}N_2O_4Na]^+$.

Supplementary Methods

Computational simulation on cluster of PCDAs. PCDA molecule was firstly built by the aid of MarvinSketch (http://www.chemaxon.com). Then it was optimized sequentially at molecular mechanical level by OPLS[1] method *via* steepest descent algorithm and Fletcher-Reeves[2] algorithm *via* employing Hyperchem[3]. Further optimization was conducted at the same level with MM+[4] method using Fletcher-Reeves algorithm at Hyperchem workspace. Optimized PCDA (shown in Fig. S1a and Fig. S1b) molecules were merged together in the workspace of Hyperchem. Langevin dynamics simulations were conducted at 300K. In this simulation, the solvent effect was implicitly considered with Charmm27 force field[5,6] and the scale factor was set to 80. Friction coefficient was from 0.05 ps^{-1} to 0.10 ps^{-1}. On the basis of those results, another PCDA cluster consisting of 16 PCDAs was constructed by merging two 2-PCDA clusters, then two 4-PCDA clusters, and finally two 8-PCDA clusters sequentially. At each stage, 100 ps Langevien dynamics simulation was conducted at 300K. Friction coefficients were set to 0.05 ps^{-1}, 0.075 ps^{-1} and 0.10 ps^{-1}, respectively.

Computational simulation on the interaction between PDA and melittin. The structure of melittin at 2.0 Å by Eisenberg, Gribskov, and Terwilliger is available in Protein Data Bank (PDB ID: 2MLT). The structure of PDA (degree of polymerization is 8) was constructed with Discover Studio 3.1[7] and optimized in Hyperchem workspace. The PDA structure was demonstrated in Fig. S3. The interaction between melittin and PDA was explored with two kinds of methods. One is to dock PDA to melittin with the help of AutoDock Vina[8] and the other is to perform simulated annealing using molecular dynamics. Before conducting a docking experiment with AutoDock Vina, receptor melittin was prepared with AutoDockTools-1.5.4 and Kollman charges[9] were assigned to all atoms of the receptor. The 3-dimensional parameters of grid box in X, Y and Z directions were set to 34Å, 28Å and 16Å, respectively. The ligand PDA was prepared by the aid of Raccoon 1.0b. Melittin is a peptide consisting of 26 amino acid residues. It is not clear where the binding site of the peptide is. Thus, it was assumed that everywhere on the surface of the peptide is the potential binding site. While preparing the receptor for docking, a big enough grid box was set to guarantee that every place on the peptide surface would be the potential binding site. Molecular dynamics simulation could facilitate modeled system to surmount small energy barriers on the potential surface and locate sites of lower potential energy[10], and dynamic annealing was often used to obtain a lower energy minimum[11]. While performing a simulated annealing using molecular dynamics on complex composed of melittin and PDA, initial conformation of the complex was obtained by randomly merging optimized PDA to melittin in the

workspace of HyperChem. Then the complex experienced a series of molecular dynamics simulations including being heated from 0K to 500K for 30 picoseconds (ps), running at 500K for 100ps, being cooled from 500K to 300K for 100ps and being equilibrated at 300K for 100ps. The temperature steps at the heating and cooling stages were set to 30 $K \cdot ps^{-1}$ and 2 $K \cdot ps^{-1}$, respectively.

Supplementary References

1 Jorgensen, W. L., Maxwell, D. S. & Tirado-Rives, J. Development and Testing of the OPLS All-Atom Force Field on conformational Energetics and Properties of Organic Liquids. *J. Am. Chem. Soc.* **118**, 11225-11236 (1996).

2 Fletcher, R. & Reeves, C. M. Function minimization by conjugate gradients. *Comput. J.* **7**, 149-154 (1964).

3 HyperChem(TM). Professional 8.0, Hypercube, Inc., 1115 NW 4th Street, Gainesville, Florida 32601, USA.

4 Allinger, N. L. Conformational analysis. 130. MM2. A hydrocarbon force field utilizing V1 and V2 torsional terms. *J. Am. Chem. Soc.* **99**, 8127-8134 (1977).

5 Brooks, B. R. *et al.* CHARMM: the biomolecular simulation program. *J. Comput. Chem.* **30**, 1545-1614 (2009).

6 Brooks, B. R. *et al.* CHARMM: A program for macromolecular energy, minimization, and dynamics calculations. *J. Comput. Chem.* **4**, 187-217 (1983).

7 Hung, D. T., Shakhnovich, E. A., Pierson, E. & Mekalanos, J. J. Small-molecule inhibitor of Vibrio cholerae virulence and intestinal colonization. *Science* **310**, 670-674 (2005).

8 Trott, O. & Olson, A. J. AutoDock Vina: improving the speed and accuracy of docking with a new scoring function, efficient optimization, and multithreading. *J. Comput. Chem.* **31**, 455-461 (2010).

9 Besler, B. H., Merz, K. M. & Kollman, P. A. Atomic charges derived from semiempirical methods. *J. Comput. Chem.* **11**, 431-439 (1990).

10 Grant, B. J., Gorfe, A. A. & McCammon, J. A. Large conformational changes in proteins: signaling and other functions. *Curr. Opin. Struct. Biol.* **20**, 142-147 (2010).

11 Levitt, M. Protein folding by restrained energy minimization and molecular dynamics. *J. Mol. Biol.* **170**, 723-764 (1983).